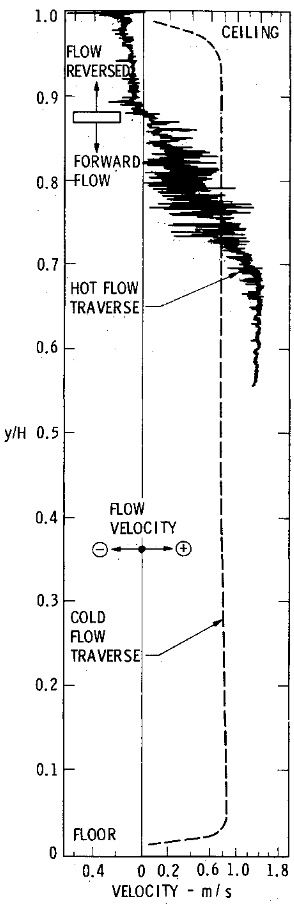

Fig. 4 Hot film anemometer traverse for test 2 conditions 30 cm upstream of fuel pan.

Table 2 Measured convective heat-transfer coefficients

	Location	
Test conditions	1	2
Near vertical plume:		
test 6 (with fence)	40–50 W/m^2·K	10–20 W/m^2·K
Slight blowing:		
tests 4 and 5	5–12 W/m^2·K	12–40 W/m^2·K
Moderate blowing:		
test 3	10–12 W/m^2·K	~5 W/m^2·K
Highly blown:		
tests 1 and 2	Negligible	<5 W/m^2·K

Conclusions

These results describe the detailed fire and flow characteristics in a one-third-scale aircraft cabin fire simulation with application to the evaluation of aircraft postcrash fire hazards. While reduced in scale, the experiment possesses key features that can be expected in the postcrash fire scenario (heat fluxes, fuel, and ventilation conditions). Assuming the same heat release rate per unit area of fuel, a fire of approximately 5 times the width (1.5 m) and heat release would possess a similar flame geometry in a full-scale cabin dimension. Flame height scales with pool width as $\sim W^{0.7}$ in this regime.[8] Of course, since momentum fluxes in the plume scale on flame height, the relative momentum fluxes of the ventilation and plume flow would be different in reduced and full-scale conditions. Nevertheless, these results show that wind-induced ventilation may significantly affect fire plume orientation, smoke transport, and heat fluxes and thus will affect subsequent fire spread and the immediate survivability of the passengers.

Acknowledgments

This work presents the results of research carried out by the Jet Propulsion Laboratory at the California Institute of Technology under contract with the National Aeronautics and Space Administration. The work was supported by the Transport Aircraft Aviation Safety Program at the Office of Aeronautics and Space Technology (OAST) of NASA. The authors acknowledge Dr. K.G. Harstad and Messrs. D.C. Schneider and J.J. Godley for their assistance in conducting the experiments.

References

[1]Sarkos, C.P., Hill, R.G., and Howell, W.D., "The Development and Application of a Full-Scale Wide-Body Test Article to Study the Behavior of Interior Materials During a Post Crash Fuel Fire," *Journal of Fire and Flammability*, Vol. 13, 1982, pp. 172–202.

[2]Parker, J.A. and Kourtides, D.A., "Fireworthiness of Transport Aircraft Interior Systems," AIAA Paper 81-1142, presented at the AIAA 16th Thermophysics Conference, Palo Alto, CA, June 23–25, 1981.

[3]Bankston, C.P. and Back, L.H., "Pool Fire-Ventilation Crossflow Experiments in a Simulated Aircraft Cabin Interior," *Journal of Aircraft*, Vol. 22, 1985, pp. 861–868.

[4]"Special Aviation Fire and Explosion Reduction (SAFER) Advisory Committee, Final Report, Vol. 1," FAA-ASF-80-4, Federal Aviation Administration, Office of Aviation Safety, Washington, DC, June 26, 1980.

[5]Bankston, C.P. and Back, L.H., "Measurements of the Response of Transport Aircraft Ceiling Panels to Fuel Fires," *Journal of Aircraft*, Vol. 23, 1986, pp. 207–212.

[6]Quintiere, J., McCaffrey, B.J., and Kashiwagi, T., "A Scaling Study of a Corridor Subject to a Room Fire," *Combustion Science and Technology*, Vol. 18, 1978, pp. 1–19.

[7]You, H.Z. and Faeth, G.M., "Ceiling Heat Transfer During Fire Plume and Fire Impingement," *Fire and Materials*, Vol. 3, 1979, pp. 140–147.

[8]Thomas, P.H., "The Size of Flames From Natural Fires," *Proceedings of the Ninth Symposium (International) on Combustion*, The Combustion Institute, Academic Press, New York, 1963, pp. 844–859.

Effect of a Round Airfoil Nose on Leading-Edge Suction

C. Edward Lan* and Ingchung Su†
University of Kansas, Lawrence, Kansas

Introduction

IT is well known that highly swept slender wings can develop a significant amount of vortex lift and drag due to lift. This vortex lift effect is, in turn, influenced by the leading-edge radius. To calculate the vortex lift effect through the suction analogy, it is necessary to predict the leading-edge suction. Most recent methods of the suction analogy to estimate the vortex force incorporate either the method of Carlson and Mack[1] or Kulfan[2,3] to determine the effect of rounded leading edges. Carlson and Mack developed an empirical method for estimation of attainable thrust and then equated the vortex force to the undeveloped thrust. On the other hand, Kulfan assumed that the vortex lift started to develop at an angle of attack (α_s) at which the nose drag is equal to the leading-edge suction.

Received Oct. 22, 1986; revision received Feb. 12, 1987.

*Professor, Department of Aerospace Engineering. Associate Fellow AIAA.

†Graduate Student.

In this Note, Kulfan's concept for an airfoil will be examined and compared with the results predicted by a theoretical airfoil aerodynamics code.[4] It will be shown that Kulfan's α_s approximately coincides with the angle of attack at which the leading-edge laminar separation first occurs.

Theoretical Method

Theoretical results are obtained with an airfoil aerodynamics program for viscous flow.[4] The position of laminar separation point is estimated by the Thwaites criterion:

$$\frac{\theta^2}{\nu}\frac{dU_e}{ds} = -0.07 \qquad (1)$$

where θ is the momentum thickness, ν the kinematic viscosity, U_e the velocity at the edge of boundary layer, and s the distance along the airfoil surface from the stagnation point. A panel method is used in the code for the inviscid flow and an integral method for the boundary layer. The interaction between the inviscid flow and boundary layer is calculated iteratively.

Based on Kulfan's concept, a flow separation angle (α_s) can be found by equating the nose drag coefficient (c_R) to the leading-edge suction coefficient (c_t). According to Ref. 5, the nose drag coefficient is equal to

$$c_R = \pi(r_0/c)/(-M_\infty^2)^{1/2} \qquad (2)$$

where r_0 is the leading-edge radius. To find the critical angle (α_s) at which $c_t = c_R$, note that

$$c_t = 2\pi[\sin\alpha + \alpha_1]^2/(1-M_\infty^2)^{1/2} \qquad (3)$$

where α_1, according to the thin airfoil theory, is given by[5]

$$\alpha_1 = -\frac{1}{\pi}\int_0^\pi \frac{dz_c}{dx} d\theta \qquad (4)$$

By equating Eqs. (2) and (3), it can be found that

$$\alpha_s = \sin^{-1}\{\pm(r_0/2_c)^{1/2} - \alpha_1\} \qquad (5)$$

Equations (3) and (5) show that for a positively cambered airfoil (i.e., α_1 being negative), c_t at a given α is reduced and α_s is increased by camber.

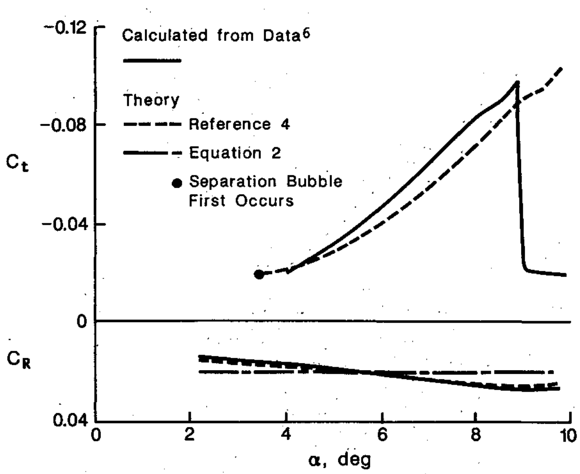

Fig. 1 Leading-edge suction on NACA 63-009 airfoil. $M = 0.17$, $Re = 5.8 \times 10^6$.

The effective suction coefficient is then calculated as

$$c_{t_{\rm eff}} = c_t, \qquad |\alpha| < |\alpha_s|$$

$$c_{t_{\rm eff}} = c_{t_s} + K[\sin(\alpha-\alpha_s)]^2, \qquad |\alpha| > |\alpha_s| \qquad (6)$$

$$K = 2\pi/(1-M_\infty^2)^{1/2}$$

where c_{t_s} is the theoretical full suction coefficient at α_s. Note that in applications to slender wing aerodynamics, only the equivalent K term in Eq. (6) in three-dimensional flow is converted to vortex lift in the suction analogy.

Results and Discussion

Experimental airfoil pressure data from Ref. 6 will be used to examine the calculation of α_s. Negative pressure is integrated to give c_t and positive pressure to c_R. The integration region covers the forward portion of the airfoil from the maximum thickness location if no separation bubble occurs. Otherwise, the integration is performed over the region forward of the separation bubble only. The results for an NACA 63-009 airfoil are presented in Fig. 1. From Fig. 1, it is seen that when the separation bubble first occurs at $\alpha = 3.5$ deg, c_t is about equal to c_R. Once massive separation occurs at $\alpha = 9$ deg, the theory will not predict the pressure distribution correctly. Additional theoretical results for this airfoil show that

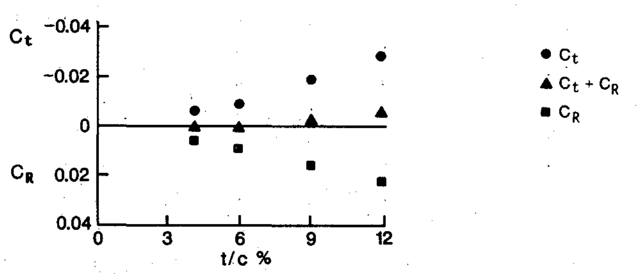

Fig. 2 Theoretical thickness effect on leading-edge suction at angles of attack at which the separation bubble first occurs on symmetrical NACA 6-series airfoils. $M = 0.17$, $Re = 5.8 \times 10^6$.

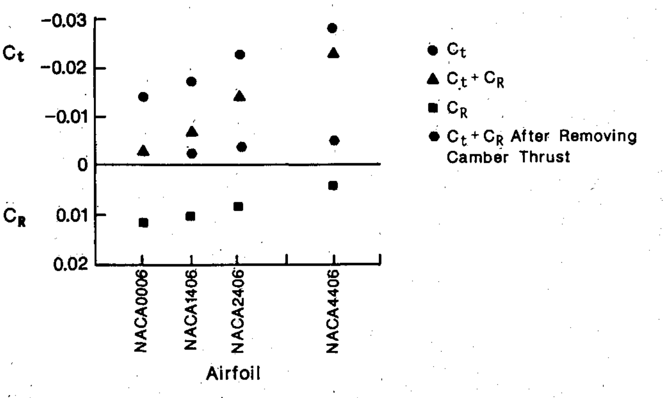

Fig. 3 Theoretical camber effect on leading-edge suction at angles of attack at which the separation bubble first occurs. $M = 0.17$, $Re = 5.8 \times 10^6$.

Table 1 Calculated angles of attack (α_s) at which laminar separation first occurs

NACA airfoil	α_s, deg Ref. 4	α_1, deg Eq. (4)	α_s, deg Eq. (5)
4406	5.0	−0.51	3.07
2406	4.0	−0.26	2.81
1406	3.5	−0.13	2.68
0006	3.0	0	2.55

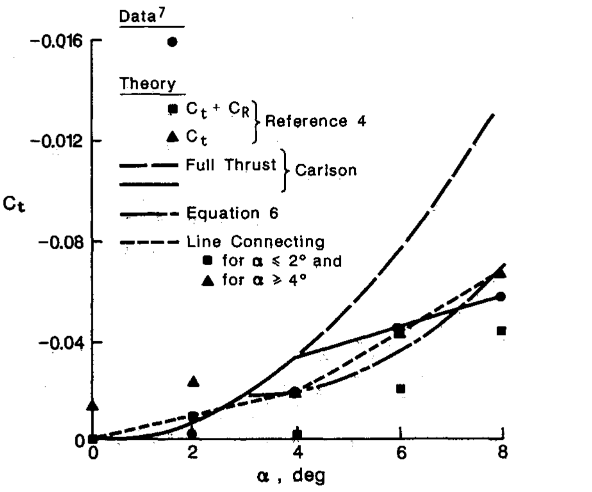

Fig. 4 Variation of leading-edge suction with angle of attack for an NACA 64A009 airfoil. $M=0.4$, $Re=0.86\times10^6$.

the values of α_s and c_t are approximately the same at Reynolds numbers equal to 5.8 and 0.58×10^6. Figure 2 shows the effect of thickness on c_t at $\alpha=\alpha_s$. Again it is seen that the sum of c_t and c_R is approximately zero for all thickness ratios examined. This is precisely Kulfan's concept. The accuracy of the concept for thick airfoils is slightly less than that for thin airfoils.

The camber effect is illustrated in Fig. 3 for four NACA four-digit airfoils. It is seen that at α_s, c_t is greater than c_R. This is due to the pressure thrust generated on the forward camber (to be called the camber thrust in the following). To remove the camber thrust in performing the pressure integration, the slope of the upper airfoil surface is reduced by the local mean line slope and that of the lower surface is increased by it. The results indicated in Fig. 3 by hexagonal symbols show that Kulfan's concept is still reasonable if camber thrust is removed from the net suction. In applications in thin airfoil or wing theory, this is usually true, because c_t as given by Eq. (3) does not contain the contribution of camber thrust.

Table 1 shows the difference in α_s predicted by the code of Ref. 4 and Eq. (5) the thin airfoil theory of Eq. (5). It is seen that α_s calculated with Eq. (5) is reasonable only if the camber is small.

To find out whether Kulfan's method is realistic for estimation of attainable thrust, theoretical c_t is compared with experimental data for an NACA 64A009 airfoil in Fig. 4. The circles represent the experimental data and the solid line is obtained by Carlson and Mack's empirical method. It is seen that in addition to the solid line, the short-dash curve matches the experimental results well. The short-dash curve is obtained by connecting the calculated results for c_t at $\alpha\geq4$ deg (triangles) and for c_t+c_R at $\alpha\leq2$ deg (squares). The squares represent the suction obtained by integrating the calculated viscous pressure over the region forward of the separation bubble. These calculated results underpredict the net leading-edge suction for $\alpha>2$ deg. Since the code of Ref. 4 cannot predict the size of the separation bubble, one possible explanation is that additional suction is present between the bubble and the maximum thickness location and is not included in the calculation. It is also seen that the short-dash curve, which represents the results obtained from the code of Ref. 4, agrees well with those based on Kulfan's method [Eq. (6)]. There is a definite reduction of c_t for any α greater than α_s (which is about 3 deg by Kulfan's method and 4 deg by Carlson and Mack's method) as compared to the theoretical full suction coefficient. This two-dimensional airfoil result is consistent with the three-dimensional concept that the leading-edge vortex on a wing with a round-nosed airfoil, once formed, would be of reduced strength relative to a thin sharp wing.

Conclusions

Kulfan assumed that the angle of attack for initial vortex separation on a slender wing with rounded leading edges could be obtained by equating the leading-edge suction and nose drag coefficients. This assumption has been examined and was shown to predict reasonably well the initial angle of attack at which laminar separation occurs near the airfoil nose. The assumption was shown to be slightly less accurate for thick or cambered airfoils. Attainable leading-edge suction estimated by Kulfan's method appeared to agree well with that obtained from an airfoil aerodynamics code and experimental data for a NACA 64A009 airfoil at $M=0.4$ and $Re=0.86\times10^6$.

Acknowledgment

This work was supported by NASA Grant NSG-1629.

References

[1]Carlson, H. W. and Mack, R. J., "Studies of Leading-Edge Thrust Phenomena," *Journal of Aircraft,* Vol. 17, Dec. 1980, pp. 890–897.

[2]Kulfan, R. M., "Wing Airfoil Shape Effects on the Development of Leading-Edge Vortices," AIAA Paper 79-1675, Aug. 1979.

[3]Kulfan, R. M., "Wing Geometry Effects on Leading Edge Vortices," AIAA Paper 79-1872, Aug. 1979.

[4]Stevens, W. A., Goradia, S. H., and Braden, J.A., "Mathematical Model for Two-Dimensional Multi-Component Airfoils in Viscous Flow," NASA CR-1843, July 1971.

[5]Robinson, A. and Laurmann, J. A., *Wing Theory,* Cambridge University Press, New York, 1956.

[6]McCullough, G. B. and Gault, D. E., "Examples of Three Representative Types of Airfoil-Section Stall at Low Speed," NACA TN 2502, Sept. 1951.

[7]Daley, B.N. and Dick, R.S., "Effect of Thickness, Camber and Thickness Distribution on Airfoil Characteristics at Mach Numbers up to 1.0," NACA TN 3607, 1956.

Residual Stresses in 2024-T81 Aluminum Using Caustics and Moiré Interferometry

Basil P. Leftheris* and Robert Schwarz†
Grumman Corporate Research Center
Bethpage, New York

Introduction

CRACK growth information is important in estimating fatigue life in aircraft structures. The interaction between existing residual stresses in aluminum alloy sheet stock and residual stresses induced by cold-working the holes is difficult to evaluate analytically, mainly because existing residual stresses are not clearly defined. However, such cases can be evaluated experimentally with fatigue specimens under cyclic loading by observing the changes in the stress intensity factor K_I during crack growth.

The method of caustics, also known as the shadow method, can be used during cyclic fatigue testing, without interrupting the test, to evaluate the stress intensity factors. We use the method of caustics to evaluate the behavior of 2024-T81 aluminum alloy sheet (0.125 in. thick) in longitudinal and long

Received Sept. 8, 1986; revision received Jan. 6, 1987.

*Principal Investigator, Senior Staff Scientist. Member AIAA.
†Engineering Specialist, Test Operations.